J. Chem. Sci. Vol. 125, No. 6, November 2013, pp. 1429–1434.

Effect of charged microenvironment on the electrochemistry of $[Fe_2S_2(OC_6H_5)_4]^{2-}$ cluster

DHANADA SARMAH and DIGANTA KUMAR DAS*
Department of Chemistry, Gauhati University, Guwahati 781 014, India
e-mail: digantakdas@gmail.com

MS received 8 April 2013; revised 23 July 2013; accepted 24 July 2013

Abstract. Although cysteine is the preferred ligand for [Fe–S] core in case of iron–sulphur proteins, presence of other ligands together with cysteine is not uncommon. Being basically electron transfer proteins, redox potential of [Fe–S] core in these proteins in crucial to their functioning. Among other factors, charged nature of the microenvironment is believed to tune the redox potential. The iron–sulphur cluster, $[Fe_2S_2(OC_6H_5)_4]^{2-}$, has been investigated electrochemically in positive and negative microenvironments, both in solution and in film. Charge nature around the active centre has been found to affect its redox potential and diffusion coefficient significantly. In a film, where charges are more localized compared to solution, the effect on redox potential was more prominent.

Keywords. Iron–sulphur proteins; cyclic voltammetry; square wave voltammetry; redox potential; film; diffusion coefficient.

1. Introduction

Iron–sulphur proteins are important components of electron transfer chains involved in a number of biological systems including respiration and photosynthesis.[1] The most common iron–sulphur clusters found as active centres in iron–sulphur proteins are $[Fe_2S_2]$, $[Fe_3S_4]$ and $[Fe_4S_4]$, in which Fe(III) ions are coordinated to cysteines from the peptide and are linked to each other through inorganic sulphur.[2] Iron–sulphur proteins with $[Fe_2S_2]$ cluster as active centre have been identified in plants, bacteria and also in mammals. This cluster is also an important constituent of a number of redox enzymes – xanthine oxidase, CO oxidase, succinate dehydrogenase and putidamonooxin.[3]

Non-cysteine ligands together with cysteine is found in an important class of iron–sulphur proteins, Rieske proteins.[4–6] Rieske proteins are found in proteins isolated from mitochondria and related redox chains, phthalate dioxygenase system from *Pseudomonas cepacia*.[6,7] Rieske centre contains $[Fe_2S_2]$ core with a pair of nonsulphur ligand histidine coordinated to one iron. The tunable range of redox potential of Rieske centre is much wider, +350 mV to −150 mV, than that of ferredoxin $[Fe_2S_2]$, where redox potential value varies from −250 mV to −420 mV.[8] Rieske centre or ferredoxin $[Fe_2S_2]$ involves two redox states interrelated by one electron transfer as: $\left[Fe^{3+}(S)_2 Fe^{3+}\right] \rightleftarrows \left[Fe^{3+}(S)_2 Fe^{2+}\right]$. Relative stability of these two states should be crucial in determining the redox potential.

Existence of non-cysteine bound $[Fe_2S_2]$ cores in Rieske type proteins has led to attempts to synthesize complexes with oxygen and nitrogen ligands. Characterized species include $[Fe_2S_2(OC_6H_5)_4]^{2-}$, $[Fe_2S_2(NC_4H_4)_4]^{2-}$, etc.[9] Studies on redox behaviour of these clusters surrounded by a hydrophobic environment are of biological significance. Electrochemistry of these clusters has elucidated that synthetic water soluble Fe–S clusters in aqueous solution exhibit more positive redox potentials than water insoluble clusters in organic solvents.[10,11] Through model studies, it has been established that microenvironment around the active centre of iron–sulphur proteins plays a vital role in determining the redox potential.[12–15]

Self-assembled monolayer (SAM) films on electrode surfaces have gained importance because of their applications in interfacial electron transfer, electrochemistry, biological membrane, catalysis, etc.[15,16] Surfactants can be adsorbed on an electrode surface to form a surfactant film.[17,18] Adsorption is through the hydrophobic surfactant tail on the electrode surface with the polar head group directed towards the bulk water phase.[19]

We report herein the effect of charge nature of microenvironment, provided by differently charged surfactants, on the redox potential of $[Fe_2S_2(OC_6H_5)_4]^{2-}$.

*For correspondence

Redox potentials of the cluster have also been reported in surfactant films in order to investigate the effect of proximity of charges on redox potential.

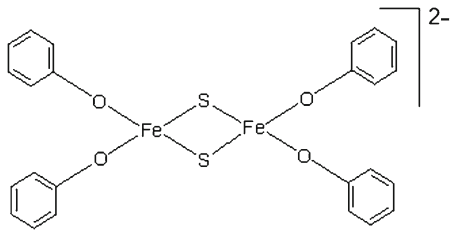

Structure of $[Fe_2S_2(OC_6H_5)_4]^{2-}$

2. Experimental

2.1 *General procedure*

All the chemicals are from Merck and used as received. Surfactants used are cetyltrimethyl-ammonium bromide (CTAB) and sodiumdodecyl sulphate (SDS). These are cationic and anionic, respectively. Surfactant solutions used are 1% (w/v) surfactant in acetonitrile (CH_3CN). Acetonitrile was distilled twice before use. CHI 600B electrochemical analyser with a three-electrode cell assembly was used. The working electrode (WE) is glassy carbon (GC) with the Ag–AgCl as reference electrode and platinum wire as auxiliary electrode. Supporting electrolyte used was 0.1 M tetrabutylammonium perchlorate (TBAP). The WE was cleaned before each run by polishing with 0.1 mM alumina using a BAS polishing kit followed by sonication. Diffusion co-efficient of the cluster on to the electrode surface has been calculated using the Cottrell equation as reported.[20] Area of the platinum electrode surface has been taken to be 0.025 cm^2.

2.2 *Preparation of film*

0.1 g of the cluster was dissolved in 10 mL CH_3CN together with 0.1 g of either CTAB or SDS. 0.5 μL of the solution was placed on the tip of GC electrode and allowed to evaporate under dry nitrogen environment in specially designed simple glassware as reported.[13] Electrochemical experiments were performed by immersing the tip of this electrode into mercaptide buffer solution (pH = 7.0) containing 0.1 M $NaNO_3$ as supporting electrolyte.

2.3 *Preparation and characterization of $[Fe_2S_2(OC_6H_5)_4]^{2-}$*

(Bu_4N) $[Fe_2S_2(OAr)_4]$ was prepared as reported[21] using Schlenk line under nitrogen environment. The cluster was found to show identical electronic spectra as reported earlier confirming its structure.[21]

3. Results and discussion

Figure 1 shows the cyclic voltammogram of $[Fe_2S_2(OC_6H_5)_4]^{2-}$ in CH_3CN at different scan rates on a GC electrode. One reduction peak followed by a redox couple was observed clearly in the cyclic voltammograms of the cluster. At scan rate 0.100 Vs^{-1}, the reduction peak was observed at −0.440 V and the reversible redox couple was observed at redox potential value of −0.840 V with separation in peak potential as 0.488 V. These redox potential values were further confirmed by square wave voltammetry experiments. The nature of the cyclic voltammogram and redox potential values are found to be similar to reported values, confirming the formation of the cluster. The irreversible reduction peak is due to 2-/3- redox couple while the quasi reversible couple is because of 3-/4- redox process. The plot of cathodic and anodic peak currents for the redox couple versus square root of scan rates is linear ($R^2 = 0.997$) confirming that the redox process is diffusion-controlled. Ratio of cathodic current to anodic current at every scan rate is *ca.* 1.0, which is characteristic of a reversible redox process (table 1).

To observe the effect of positive microenvironment on the redox potentials of $[Fe_2S_2(OC_6H_5)_4]^{2-}$, its cyclic voltammograms were recorded at different scan rates in 1% (w/v) solution of CTAB in CH_3CN (figure 2a). The irreversible reduction peak was found to shift in positive direction to −0.425 V. Redox potential of the reversible couple was found to shift to −0.795 V.

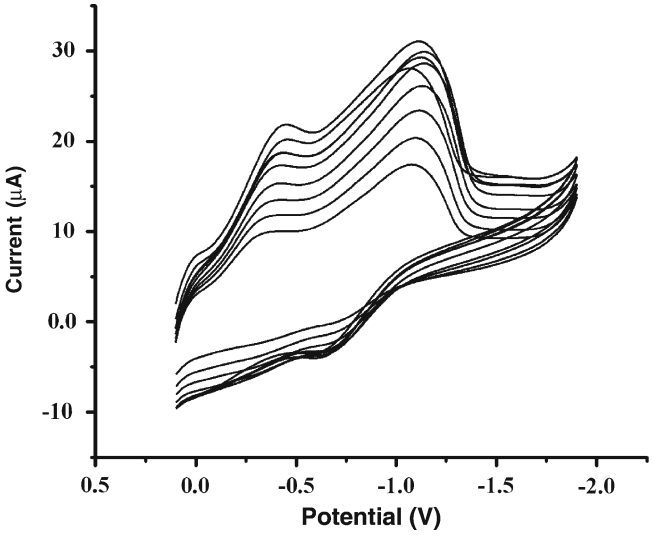

Figure 1. Cyclic voltammogram of $[Fe_2S_2(OC_6H_5)_4]^{2-/3-}$ redox process (irreversible reduction peak) and $[Fe_2S_2(OC_6H_5)_4]^{3-/4-}$ redox process (reversible redox couple) in CH_3CN at scan rates of 0.20 to 0.90 Vs^{-1} at an interval of 0.10 Vs^{-1} (WE=GC, RE=Ag–AgCl (3M NaCl), 0.1 M TBAP).

Table 1. Electrochemical results of $[Fe_2S_2(OC_6H_5)_4]^{2-}$ in different medium.

	$E_{1/2}$ (V)				
	CV		SWV		
Medium	(2-/3-)	(3-/4-)	(2-/3-)	(3-/4-)	D_o (cm^2s^{-1})
CH_3CN	−0.440 V,	−0.840 V	−0.442,	−0.843	2.22×10^{-8}
CH_3CN/CTAB	−0.425 V,	−0.795 V	−0.423,	−0.798	2.77×10^{-7}
CH_3CN/SDS	−0.600 V,	−0.950 V	−0.600,	−0.952	1.62×10^{-8}
SDS Film	−0.400 V,	−0.720 V	−0.403,	−0.724	–
CTAB Film	–	−0.145 V	–	−0.148	–

Diffusion coefficients (D_o) are for $[Fe_2S_2(OC_6H_5)_4]^{3-}$ state. The WE is GC disc for solution studies and films were cast on GC electrode surface (RE = Ag–AgCl, 3M NaCl).

Hence, presence of cationic CTAB could impart a positive shift of 0.025 V on the irreversible reduction peak and 0.045 V on the redox potential of the reversible redox couple. The plot of cathodic and anodic currents versus square root of scan rate was found to be linear ($R^2 = 0.991$). Redox potential obtained was confirmed by square wave voltammetry (figure 2b).

Cyclic voltammograms of $[Fe_2S_2(OC_6H_5)_4]^{2-}$ in CH_3CN containing 1% (w/v) anionic SDS at different scan rates were also recorded (figure 3) in order to investigate the effect of negative microenvironment on redox potentials. Cyclic voltammogram similar to that of CH_3CN was observed consisting of one reduction peak and a quasi reversible redox couple. The plot of redox currents versus square root of scan rates was found to be linear ($R^2 = 0.994$). The reduction peak was shifted to −0.600 V, which is 0.160 V more negative compared to that of CH_3CN. Redox potential of the quasi reversible couple was also shifted by 0.100 V in negative direction to −0.950 V.

The positive shift of 0.025 V on the irreversible reduction peak and 0.045 V on the redox potential of the quasi reversible redox couple could be explained by the fact that cationic CTAB surfactants relatively stabilize the more negative states in case of 2-/3- and 3-/4- redox couples. This should make reduction processes relatively easier and hence positive shift in the potentials was observed. On the other hand, presence of negative SDS molecules make the less negative states relatively more stable compared to more negative ones resulting in relatively difficult reduction processes and hence the negative shift.

Cyclic voltammograms were also recorded for $[Fe_2S_2(OC_6H_5)_4]^{2-}$ encapsulated in CTAB and SDS film on GC electrode surface. In case of CTAB film, only a quasi reversible redox couple due to $[Fe_2S_2(OC_6H_5)_4]^{3-/4-}$ was observed and the irreversible reduction due to $[Fe_2S_2(OC_6H_5)_4]^{2-/3-}$ has not been observed. Figure 4a shows the cyclic voltammograms of $[Fe_2S_2(OC_6H_5)_4]^{3-/4-}$ at different scan rates

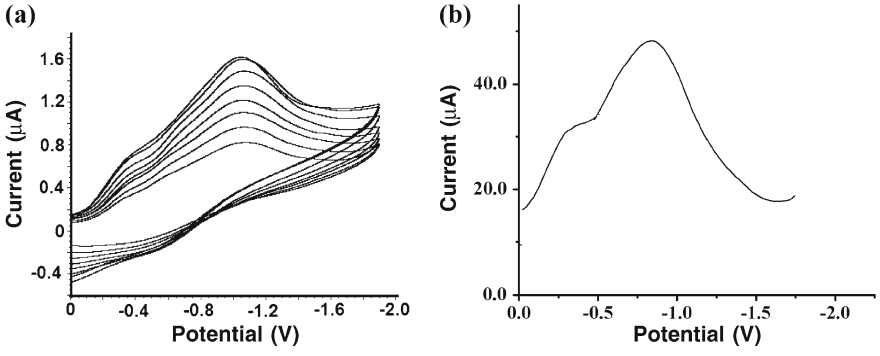

Figure 2. (**a**) Cyclic voltammogram of $[Fe_2S_2(OC_6H_5)_4]^{2-/3-}$ redox process (irreversible reduction peak) and $[Fe_2S_2(OC_6H_5)_4]^{3-/4-}$ redox process (reversible redox couple) in 3% (w/v) CTAB/CH_3CN at scan rates of 0.20 to 0.90 Vs^{-1} at an interval of 0.10 Vs^{-1}. (**b**) Square wave voltammogram of $[Fe_2S_2(OC_6H_5)_4]^{2-/3-}$ and $[Fe_2S_2(OC_6H_5)_4]^{3-/4-}$ redox process in 3% (w/v) CTAB/CH_3CN (B) (WE=GC, RE=Ag–AgCl (3M NaCl), 0.1 M TBAP).

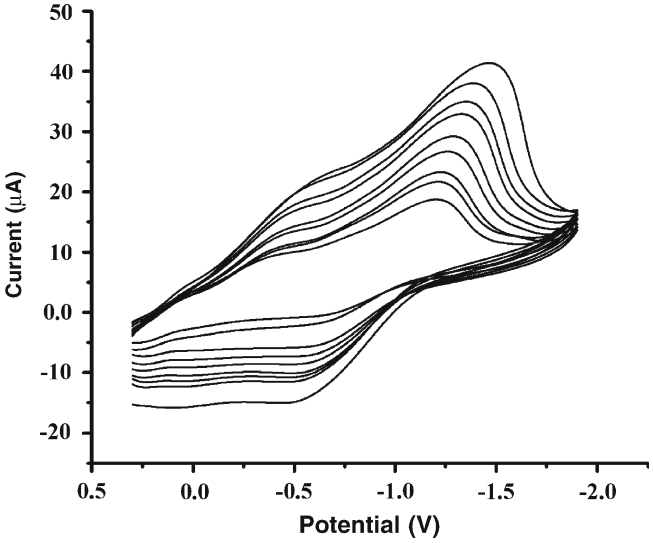

Figure 3. Cyclic voltammogram of $[Fe_2S_2(OC_6H_5)_4]^{2-/3-}$ redox process (irreversible reduction peak) and $[Fe_2S_2(OC_6H_5)_4]^{3-/4-}$ redox process (reversible redox couple) in 3% (w/v) SDS/CH_3CN at scan rates of 0.20 to 0.90 Vs^{-1} at an interval of 0.10 Vs^{-1} (WE=GC, RE=Ag–AgCl (3M NaCl), 0.1 M TBAP).

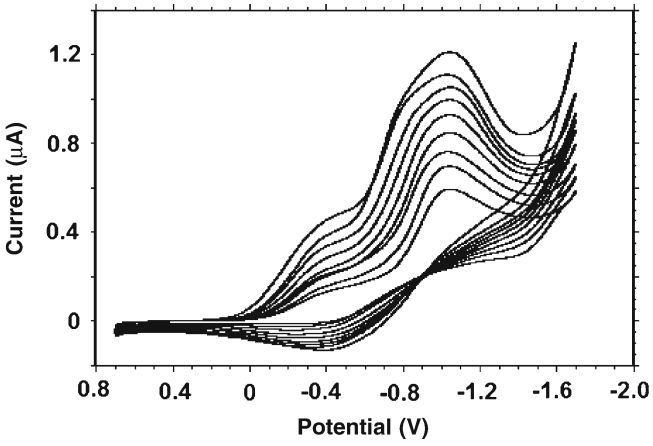

Figure 5. Cyclic voltammogram of $[Fe_2S_2(OC_6H_5)_4]^{2-/3-}$ redox process (irreversible reduction peak) and $[Fe_2S_2(OC_6H_5)_4]^{3-/4-}$ redox process (reversible redox couple) in SDS film on GC electrode surface at scan rates of 0.20 to 0.90 Vs^{-1} at an interval of 0.10 Vs^{-1}. The $[Fe_2S_2(OC_6H_5)_4]^{1-/2-}$ redox process was not observed (WE=GC, RE=Ag–AgCl (3M NaCl), 0.1 M $NaNO_3$ in mercaptide buffer).

in CTAB film. Redox potential value was found to be −0.145 V and this potential value is 0.650 V more positive than that of CTAB/CH_3CN medium. Redox potential value was also confirmed by square wave voltammetry (figure 4b). In the film, the positive charges of CTAB are in (i) greater proximity towards $[Fe_2S_2(OC_6H_5)_4]^{2-/3-\text{ and }3-/4-}$ couple and (ii) are static compared to dynamic positives charges of CTAB in CH_3CN/CTAB medium. Therefore, in film $[Fe_2S_2(OC_6H_5)_4]^{2-/3-\text{ and }3-/4-}$ should experience more influence from CTAB compared to CTAB in CTAB/CH_3CN medium.

In SDS film, the cyclic voltammogram showed the irreversible reduction peak as well as the redox couple similar to the ones in SDS/CH_3CN medium (figure 5). The irreversible reduction peak was observed at −0.400 V and the redox couple was observed with redox potential value of −0.720 V. Redox potential due to the reversible couple is 0.575 V negative compared to that in CTAB film. This result is expected for the cluster inside a negatively charged film.

Double potential step chrono coulometry experiments were performed for $[Fe_2S_2(OC_6H_5)_4]^{3-/4-}$ in CH_3CN, CTAB/CH_3CN and SDS/CH_3CN media as well as CTAB and SDS films using 25 mV pulse for 0.25 s. Figure 6 compares the charge versus time profile

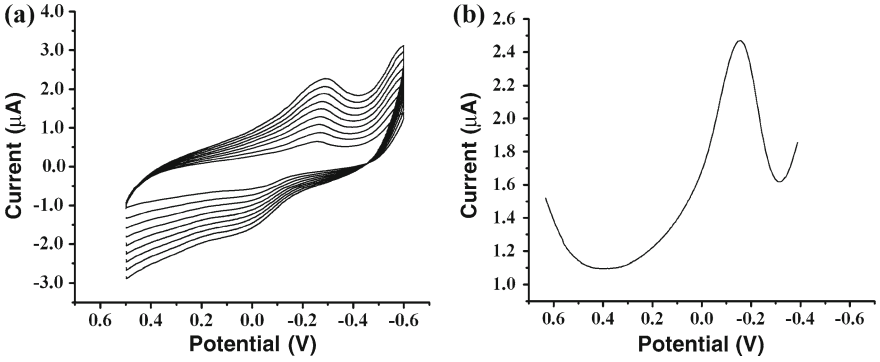

Figure 4. (**a**) Cyclic voltammograms of $[Fe_2S_2(OC_6H_5)_4]^{2-/3-}$ redox process in CTAB film on GC electrode surface at scan rates of 0.20 to 0.90 Vs^{-1} at an interval of 0.10 Vs^{-1}. (**b**) Square wave voltammogram of $[Fe_2S_2(OC_6H_5)_4]^{3-/4-}$ redox process in CTAB film on GC electrode surface. The $[Fe_2S_2(OC_6H_5)_4]^{1-/2-}$ redox process was not observed (WE=GC, RE=Ag–AgCl (3M NaCl), 0.1 M $NaNO_3$ in mercaptide buffer).

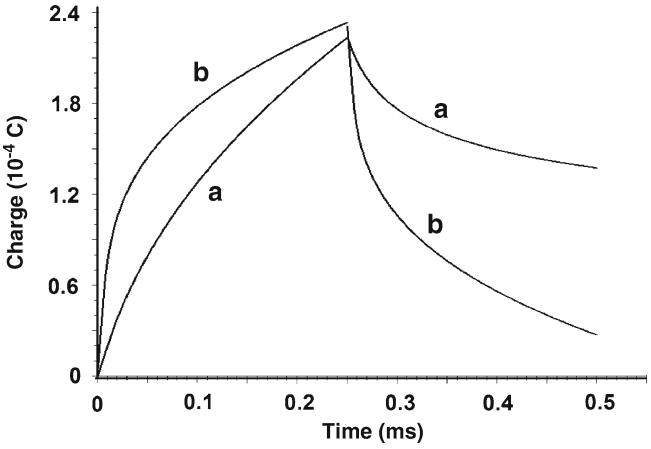

Figure 6. The charge versus time response of double potential step chronocoulometry of $[Fe_2S_2(OC_6H_5)_4]^{3-/4-}$ redox process in (a) CTAB/CH_3CN (WE: Pt disc, RE=Ag–AgCl (3M NaCl), 0.1 M TBAP) and (b) CTAB film on GC electrode surface (RE=Ag–AgCl, 3M NaCl, 0.1 M $NaNO_3$ in mercaptide buffer).

for $[Fe_2S_2(OC_6H_5)_4]^{3-/4-}$ in CH_3CN/CTAB and CTAB films. The charge versus time profile is typical for that of diffusion-controlled process for $[Fe_2S_2(OC_6H_5)_4]^{3-/4-}$ in CH_3CN/CTAB. In CTAB film, a sharper decrease in charge, compared to that in CTAB/CH_3CN, is expected for surface-confined molecules.

Diffusion coefficient for the reduced species has been calculated from the plot of current versus square root of scan rates[20] and found to be: $2.22 \times 10^{-8}\,cm^2s^{-1}$ (CH_3CN), $2.77 \times 10^{-7}\,cm^2s^{-1}$ (CTAB/CH_3CN) and $1.62 \times 10^{-8}\,cm^2s^{-1}$ (SDS/CH_3CN). Hence, in CTAB/CH_3CN, the diffusion coefficient is an order of magnitude 10 times smaller than that in CH_3CN and SDS/CH_3CN. Electrostatic attraction between the negative charge of the cluster and the positive polar heads of CTAB retards the rate of diffusion of the cluster onto the electrode surface. On the other hand, repulsion between the negative charge on the cluster and the negative polar head group of SDS helps diffusion. Higher diffusion co-efficient observed in CH_3CN compared to that in SDS/CH_3CN is due to lower viscosity of CH_3CN compared to SDS/CH_3CN.

3.1 *Comparison of redox potential of* $[Fe_2S_2(OC_6H_5)_4]^{2-}$ *with other iron–sulphur clusters*

Effect of charged microenvironment on redox potential has already been reported for other [Fe–S] cores such as – $[Fe_4S_4(SPh)_4]^{2-}$ and $[Fe_4S_4(SCH_2CH_2COO)_4]^{2-}$.[13,14] In case of $[Fe_4S_4(SPh)_4]^{2-}$, compared to the solvent dimethylformamide (DMF), in CTAB/DMF, the redox potential was 0.060 V more positive; while in SDS/DMF, it was only 0.030 V more negative. The total span in redox potential between positive and negative microenvironment is 0.090 V. In case of $[Fe_4S_4(SCH_2CH_2COO)_4]^{6-}$, redox potential could be tuned by only 0.047 V (−0.690 V and −0.737 V in CTAB and SDS micelles, respectively) by changing the microenvironment from positive to negative. These values are much smaller compared to the change in redox potential value of 0.175 V for $[Fe_2S_2(OC_6H_5)_4]^{2-}$ induced by changed microenvironment charge. The coordination of O to the $[Fe_2S_2]^{2+}$ core in $[Fe_2S_2(OC_6H_5)_4]^{2-}$ might be responsible for its wider redox potential range compared to other ones, where the [Fe–S] cores are linked by S of the ligand. This may be one of the reasons why nature has selected two non-cysteine amino acids, to be coordinated to the [Fe–S] core, for Rieske centre in order to have a much wider redox potential range of 0.500 V compared to 0.200 V range for normal $[Fe_2S_2]$ ferredoxins.[3,8]

4. Conclusion

We have shown that redox potential of $[Fe_2S_2(OC_6H_5)_4]^{2-}$ is significantly affected by the charged microenvironment provided by surfactants. Positive microenvironment shifts the redox potential in positive direction while negative microenvironment shifts it in negative direction. Diffusion coefficient of the reduced state of the cluster was 10 times smaller in cationic environment than in anionic one. This study supports nature's selection of non-cysteine amino acid in the active centre of Rieske proteins.

Acknowledgements

This work was supported by the University Grants Commission (UGC), New Delhi vide project No. 39/803/2010. The Department of Science and Technology (DST), New Delhi is thanked for the electrochemical analyser under FIST program.

References

1. Béatrice P and Frédéric B 2010 *Nature Rev. Microbiol.* **8** 436
2. Beinert H, Holm R H and Münck E 1997 *Science* **277** 653
3. Bertini I, Gray H B, Lippard S J and Valentine J S 1998 *Bioinorganic chemistry* (New Delhi: Viva Publishing) 365
4. Paternack R F, Gibbs E J and Villafranka J J 1983 *Biochemistry* **22** 2406

5. Hellman J D, Ballard B T and Walsh C T 1990 *Science* **248** 946
6. Griffin J H and Dervan P B 1987 *J. Am. Chem. Soc.* **109** 6840
7. Bagg A and Neilands J B 1987 *Microbiol. Rev.* **109** 6840
8. Trumpower B L 1981 *Biochim. Biophys. Acta* **639** 129
9. Coucovanis D 1984 *J. Am. Chem. Soc.* **106** 6081
10. Nakamoto M, Tanaka K and Tanaka T 1988 *Bull. Chem. Soc. Jpn.* **61** 4099
11. Okuno Y, Uoto K, Yonemitsu O and Tomohiro T 1987 *Chem. Commun.* 1018
12. Roy R C, Das D K and Das B 2007 *Indian J. Chem.* **46A** 1252
13. Roy R C and Das D K 2005 *J. Chem. Sci.* **117** 657
14. Roy R C and Das D K 2005 *Indian J. Chem.* **44A** 1597
15. Caldwell W B, Campbell D J, Chen K, Herr B R, Mirkin C A, Malik A, Durbin M K, Dutta P and Huang K G 1995 *J. Am. Chem. Soc.* **117** 6071
16. Nuzzo R G and Allara D L 1983 *J. Am. Chem. Soc.* **105** 4481
17. Lyones M E G, Breen W and Carridy I 1991 *J. Chem. Soc. Faraday Trans.* **87** 113
18. Attwood D and Florence A T 1983 *Surfactant systems – Their chemistry, pharmacy and biology* (London: Chapman and Hall), ch. 1
19. Wen X-lin, Han Z-Xu, Ricker A and Liu Z-Li 1997 *J. Chem. Res.* (*S*) 108
20. Bard A J and Faukner L R 1980 *Electrochemical methods: Fundamentals and applications* (New York: Wiley), ch. 12, p. 231
21. Cleland W E Jr and Averill B A 1984 *Inorg. Chem.* **23** 4192